# C18:3-GM1a induces apoptosis in Neuro2a cells: enzymatic remodeling of fatty acyl chains of glycosphingolipids

**Tetsuto Nakagawa, Akio Morotomi, Motohiro Tani, Noriyuki Sueyoshi, Hironobu Komori, and Makoto Ito[1]**

Department of Bioscience and Biotechnology, Graduate School of Bioresource and Bioenvironmental Sciences, Kyushu University, 6-10-1, Hakozaki, Higashi-ku, Fukuoka 812-8581, Japan

**Abstract GM1a [Galβ1-3GalNAcβ1-4(NeuAcα2-3)Galβ1-4Glcβ1-1Cer] is known to support and protect neuronal functions. However, we report that α-linolenic acid-containing GM1a (C18:3-GM1a), which was prepared using the reverse hydrolysis reaction of sphingolipid ceramide *N*-deacylase, induced apoptosis in neuronal cells. Intranucleosomal DNA fragmentation, chromatin condensation, and caspase activation, all typical features of apoptosis, were observed when mouse neuroblastoma Neuro2a cells were cultured with C18:3-GM1a but not GM1a containing stearic acid (C18:0) or oleic acid (C18:1). The phenotype of Neuro2a cells induced by C18:3-GM1a was similar to that evoked by lyso-GM1a. However, lyso-GM1a caused a complete disruption of lipid microdomains of Neuro2a cells and hemolysis of sheep erythrocytes, whereas C18:3-GM1a did neither. C18:3-GM1a, but not lyso-GM1a, was found to be abundant in lipid microdomains after the removal of loosely bound GM1a by BSA. The activation of stress-activated protein kinase/c-Jun N-terminal kinase in Neuro2a cells was observed with lyso-GM1a but not C18:3-GM1a. These results indicate that the mechanism of apoptosis induced by C18:3-GM1a is distinct from that caused by lyso-GM1a. This study also clearly shows that fatty acid composition of gangliosides significantly affected their pharmacological activities when added to the cell cultures and suggests why naturally occurring gangliosides do not possess polyunsaturated fatty acids as a major constituent.**—Nakagawa, T., A. Morotomi, M. Tani, N. Sueyoshi, H. Komori, and M. Ito. **C18:3-GM1a induces apoptosis in Neuro2a cells: enzymatic remodeling of fatty acyl chains of glycosphingolipids. *J. Lipid Res.* 2005.** 46: **1103–1112.**

**Supplementary key words** ganglioside • polyunsaturated fatty acids • neuroblastoma • lipid microdomain

Glycosphingolipids (GSLs), found in the outer leaflet of the plasma membranes of vertebrates, are thought to play functional roles in various cellular events, such as cell proliferation and differentiation (1–6) and cellular interaction and recognition, including microbial infection (7–9). There is much evidence that sphingolipids dynamically cluster with cholesterol to form lipid microdomains, so-called detergent-insoluble membranes (DIMs), detergent-insoluble GSL-enriched domains, GSL-enriched membranes, or rafts (10–12). Lipid microdomains have specific proteins that are anchored to membranes by saturated acyl chains (e.g., Src family protein tyrosine kinases and glycosylphosphatidylinositol-anchored proteins) (13). Most sphingolipids have saturated fatty acyl chains, whereas glycerophospholipids are rich in unsaturated fatty acyl chains. This allows sphingolipids to pack tightly with cholesterol to form domains in the glycerophospholipid bilayer and provides sphingolipids with their high melting temperature (14). However, the question of why cells do not synthesize GSLs with polyunsaturated fatty acids as a major constituent has not been answered.

Exogenously added GSLs, especially gangliosides, sialic acid-containing GSLs, show various biological activities in neuronal cells. For example, neurite formation, a typical phenotype for neuronal differentiation, can be induced by gangliosides, notably by GM1a [Galβ1-3GalNAcβ1-4(NeuAcα2-3)Galβ1-4Glcβ1-1Cer] (5) and GQ1b (1). Antiapoptotic effects of GM1a have also been observed (15). For the past decade, clinical applications of GM1a for neurological disorders such as Alzheimer's disease (16), Parkinson's disease (17), and spinal cord injury (18) have been reported. However, these studies and clinical applications did not focus on the role of the ceramide (Cer) moiety of gangliosides in the activity. On the other hand, GSLs are known to show heterogeneity not only in their carbohydrate moiety but also in their lipid moiety. For ex-

*Manuscript received 27 December 2004 and in revised form 28 February 2005.*

*Published, JLR Papers in Press, March 16, 2005.*
*DOI 10.1194/jlr.M400516-JLR200*

Abbreviations: Cer, ceramide; CTB, cholera toxin B-subunit; DIM, detergent-insoluble membrane; ERK, extracellular signal-regulated kinase; ESI-LC-MS, electrospray ionization-liquid chromatography-mass spectrometry; GM1a, Galβ1-3GalNAcβ1-4(NeuAcα2-3)Galβ1-4Glcβ1-1Cer; GSL, glycosphingolipid; MAPK, mitogen-activated protein kinase; NCAM, neural cell adhesion molecule; SAPK/JNK, stress-activated protein kinase/c-Jun N-terminal kinase; SCDase, sphingolipid ceramide *N*-deacylase.

[1] To whom correspondence should be addressed.
e-mail: makotoi@agr.kyushu-u.ac.jp

ample, gangliosides from bovine brain contain more than seven species of fatty acids in the Cer moiety, although stearic acid (C18:0) is a major constituent (19). Recently, it was suggested that the structure of Cer, especially the composition of fatty acids, could influence the localization and functions of GSLs on plasma membranes, possibly by direct interaction with membrane proteins, cholesterol, and phospholipids (20, 21). Thus, the function of exogenously added GSLs could be changed with the conversion of their fatty acid moiety. The present study indicates that remodeling of fatty acyl chains of GSLs is easily performed by sphingolipid ceramide *N*-deacylase (SCDase), an enzyme capable of catalyzing reversible reactions by which the *N*-acyl linkage of Cer in GSLs is hydrolyzed or synthesized (22, 23).

Lysosphingolipids, which lack fatty acyl chains of sphingolipids, are known to be accumulated in some cases of sphingolipid storage diseases (24–27). We have reported that lysosphingolipids including lyso-GM1a induced apoptosis in mouse neuroblastoma Neuro2a cells and suggested that the accumulation of lysosphingolipids, but not parental sphingolipids, triggers the apoptotic cascade in neuronal cells of patients with sphingolipidosis (28). We found in this study that GM1a containing α-linolenic acid (C18:3-GM1a) also induces apoptosis in Neuro2a cells. The fact that lyso- and PUFA-containing gangliosides showed strong cell toxicity may partly explain why cells do not synthesize these aberrant gangliosides as a major constituent. The physiological relevance of lyso-GSLs has been studied by many researchers (28–30), whereas that of PUFA-containing gangliosides has not yet been clarified, although the latter gangliosides have actually been detected as a minor constituent of various tissues (31–33). We report here that exogenously added C18:3-GM1a was abundant in the lipid microdomains, whereas lyso-GM1a disrupted them, both leading to apoptosis but in a different manner.

## MATERIALS AND METHODS

### Materials

GM1a was prepared from bovine brain gangliosides using the sialidase-producing marine bacterium *Pseudomonas* sp. YF-2 as described previously (34). Stearic acid (C18:0), oleic acid (C18:1 n-9), linoleic acid (C18:2 n-6), α-linolenic acid (C18:3 n-3), eicosapentaenoic acid (C20:5 n-3), and docosahexaenoic acid (C22:6 n-3) were obtained from Sigma (St. Louis, MO). SCDase was prepared from the culture supernatant of *Pseudomonas* sp. TK4 as described (22, 35) or purchased from Takara Bio (Otsu, Japan). Lyso-GM1a was prepared from GM1a using SCDase (36) or the SCDase-producing *Pseudomonas* sp. TK4 as a microbial catalyst, as reported previously (37). N-2 supplement was purchased from Invitrogen (Carlsbad, CA). [$^3$H]thymidine and ECL Plus reagents were purchased from Amersham Biosciences (Little Chalfont, UK). [$^{14}$C]stearic acid and [$^{14}$C]linolenic acid were purchased from American Radiolabeled Chemicals (St. Louis, MO). Ac-DEVD-MCA and zVAD-fmk were obtained from Peptide Institute, Inc. (Minoh, Japan). Specific polyclonal antibodies directed at extracellular signal-regulated kinase (ERK) 1/2, p44/42 mitogen-activated protein kinase (MAPK), phospho-ERK, and phospho-SAPK/JNK (stress-activated protein kinase/c-Jun N-terminal kinase) were obtained from Cell Signaling Technology (Beverly, MA), and monoclonal antibody (clone N-CAM 13) directed toward neural cell adhesion molecule (NCAM) was from BD Biosciences PharMingen (San Diego, CA). OptiPrep was purchased from Nycomed Pharma (Oslo, Norway).

### Synthesis and purification of the reconstructed GM1a with a single fatty acid molecule

Ten micromoles of lyso-GM1a and 25 μmol of fatty acid were incubated at 37°C for 18 h with 100 mU of SCDase in 40 ml of 25 mM phosphate buffer, pH 7.0, containing 0.1% Triton X-100. The reaction mixture was applied to a Sep-Pak Plus C18 cartridge to remove salts that had been previously equilibrated with distilled water. After a wash with 20 ml of distilled water, the GM1a was eluted from the cartridge with 1 ml of methanol and 10 ml of chloroform-methanol (2:1, v/v). The eluate was dried under $N_2$ gas, dissolved in chloroform-methanol-distilled water (65:25:4, v/v), and purified by normal-phase HPLC using a silica column (AQUASIL SS-1251, 4.6 × 250 mm, Senshu Pak; Senshu Scientific Co., Tokyo, Japan) with a linear gradient of chloroform-methanol-distilled water from 65:25:4 (v/v) to 5:4:1 (v/v). In a typical experiment, 5 μmol of C18:3-GM1a was obtained when 25 μmol of α-linolenic acid and 10 μmol of lyso-GM1a were used as the substrates.

### Electrospray ionization-liquid chromatography-mass spectrometry

Fifty nanomoles of the reconstructed GM1a was analyzed by electrospray ionization-liquid chromatography-mass spectrometry (ESI-LC-MS) with an API 365 (Applied Biosystems, Foster City, CA). The GM1a was introduced into the equipment with 50% methanol containing 5 mM ammonium acetate as a solvent at a flow rate of 5 μl/min. The mass spectrometer was operated in the positive-ion mode (the ion-spray voltage was set at 5,000 V, and the orifice voltage was 60 V).

### Cell culture

Neuro2a cells were cultured in DMEM supplemented with 60 mg/l kanamycin and 10% FBS at 37°C in an atmosphere of 95% air and 5% $CO_2$.

### DNA fragmentation, chromatin condensation, and nuclear fragmentation analyses

DNA fragmentation was analyzed by agarose gel electrophoresis. In brief, fragmented genomic DNA was extracted by incubating cells in a 10 mM Tris-HCl buffer, pH 7.5, containing 10 mM EDTA and 0.5% Triton X-100 at 4°C for 10 min. Under these conditions, intact genomic DNA was not extracted. The cell suspension was centrifuged at 15,000 rpm for 20 min, and the resulting supernatants were incubated at 37°C for 1 h in the presence of RNase A (400 μg/ml) and then for an additional 1 h in the presence of proteinase K (400 μg/ml). The fragmented DNA was precipitated with isopropanol and then analyzed by 2% agarose gel electrophoresis. For analyses of chromatin condensation and nuclear fragmentation, the cells were washed with PBS and fixed in a 1% glutaraldehyde solution at 4°C for 75 min. After fixation, cells were collected by centrifugation at 800 × *g* for 5 min, washed with PBS two times, and resuspended in PBS. The cell nuclei were stained with Hoechst 33258 (Wako, Osaka, Japan) and examined with a fluorescence microscope with an ultraviolet combination filter. The DNA fragmentation was also determined by flow cytometer (EPICS XL; Beckman Coulter, Fullerton, CA).

### Cholera toxin staining and fluorescence microscopy

Neuro2a cells, cultured on a cover glass, were treated with 40 μM GM1a for given periods in serum-free DMEM containing 20

μg/ml BSA and the N-2 supplement. To remove the GM1a loosely attached to cell surfaces, the cells were washed with DMEM containing 0.2% fatty acid-free BSA. After BSA treatment, cells were fixed with 3% paraformaldehyde in PBS for 15 min. After being rinsed with PBS and 0.1 M glycine in PBS, cells were permeabilized with 0.1% digitonin in PBS. After treatment with blocking buffer (5% skim milk in PBS) for 15 min, the samples were incubated with biotin-labeled cholera toxin B-subunit (CTB; diluted 1:1,000 with blocking buffer) at 4°C overnight followed by Cy3-labeled streptavidin at room temperature for 2 h. Samples were examined with a confocal laser-scanning microscope (Digital Eclipse C1; Nikon, Tokyo, Japan).

### SDS-PAGE and Western blotting

SDS-PAGE was carried out according to the method of Laemmli (38). Protein transfer onto a polyvinyl difluoride membrane was performed using a Trans-Blot SD Semi-Dry Cell (Bio-Rad, Hercules, CA). After treatment with 3% skim milk in TBS containing 0.1% Tween 20 (T-TBS) for 1 h, the membrane was incubated with primary antibody at 4°C overnight. After three washes with T-TBS, the membrane was incubated with horseradish peroxidase-conjugated secondary antibody at room temperature for 2 h. After another three washes with T-TBS, the ECL reaction was performed for 5 min as recommended by the manufacturer, and chemiluminescent signals were visualized on an ECL™ Minicamera (Amersham Biosciences).

### TLC blotting

After sucrose density gradient centrifugation, fractions were dialyzed with distilled water, dried with a SpeedVac concentrator, and applied to a plastic TLC plate (Polygram SIL G; Macherey-Nagel, Duren, Germany), which was developed with chloroform/methanol/0.02% $CaCl_2$ (5:4:1, v/v). After treatment with 1% skim milk in TBS for 1 h, the plate was washed three times with T-TBS and incubated with biotin-labeled CTB in TBS at room temperature for 1 h. After another three washes with T-TBS, the membrane was incubated with alkaline phosphatase polymer-conjugated streptavidin at room temperature for 1 h. After still another three washes with T-TBS, the GM1a was visualized with nitroblue tetrazolium chloride and 5-bromo-4-chloro-3-indolyl phosphate as a substrate (Roche, Basel, Switzerland).

### Sucrose and OptiPrep density gradient analyses

Sucrose gradient analysis was performed by the method described previously (39). Briefly, Neuro2a cells cultured in a 35 mm dish ($1 \times 10^6$) were suspended in 250 μl of ice-cold homogenizing buffer (10 mM Tris-HCl, pH 7.5, containing 150 mM NaCl, 5 mM EDTA, 5 μg/ml leupeptin, 5 μg/ml pepstatin, and 5 μg/ml chymostatin) containing 1% Triton X-100, allowed to stand for 20 min on ice, and homogenized using a Teflon glass homogenizer. The cell lysate was centrifuged for 5 min at 1,300 *g* and 4°C to remove nuclei and large cellular debris. The supernatant fraction was mixed with an equal volume of the homogenizing buffer containing 85% sucrose (w/v). A discontinuous sucrose concentration gradient, 1.1 ml of 30% and 0.6 ml of 5% sucrose in the same buffer, was layered over the lysate. Samples were centrifuged at 200,000 *g* for 18–20 h at 4°C. After centrifugation, 220 μl fractions were collected from the top of the gradient (10 fractions) and subjected to trichloroacetic acid precipitation. OptiPrep gradient analysis was performed as described previously with some modifications (40). The cell lysate was centrifuged at 1,300 *g* for 5 min at 4°C to remove nuclei and large cellular debris. The supernatant fraction was mixed with an equal volume of 50% (v/v) OptiPrep in the homogenizing buffer. A discontinuous OptiPrep concentration gradient, 1.1 ml of 20% and 0.6 ml of 10% OptiPrep in the same buffer, was layered over the lysate. Samples were centrifuged at 200,000 *g* for 18–20 h at 4°C. After centrifugation, 220 μl fractions were collected from the top of the gradient (10 fractions) and subjected to trichloroacetic acid precipitation.

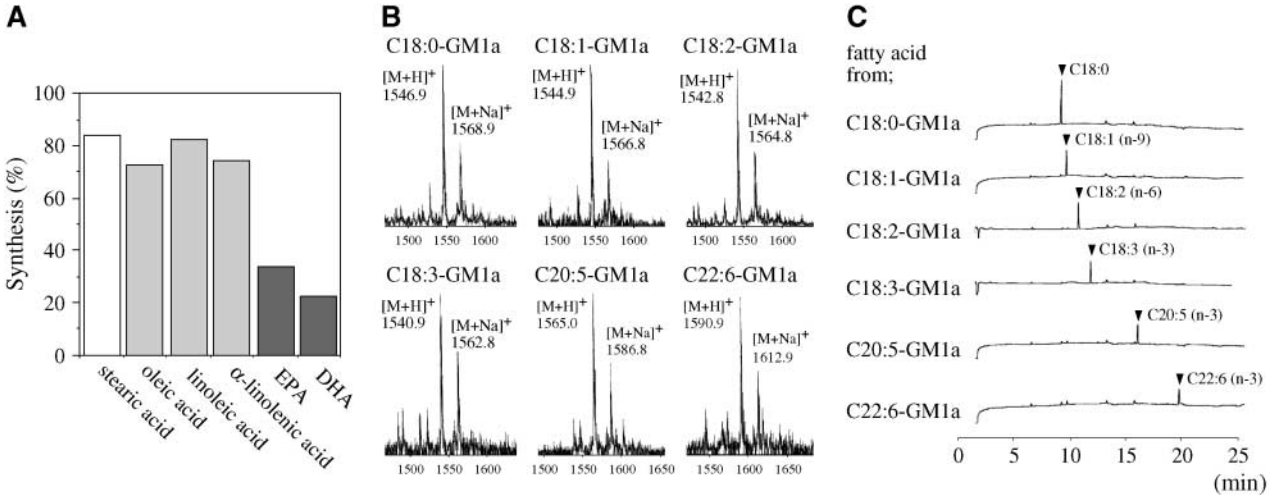


**Fig. 1.** Enzymatic synthesis of GM1a [Galβ1-3GalNAcβ1-4(NeuAcα2-3)Galβ1-4Glcβ1-1Cer] having different fatty acyl chains by sphingolipid ceramide *N*-deacylase (SCDase). A: Four nanomoles of lyso-GM1a was incubated with 10 nmol of various fatty acids at 37°C for 18 h with 40 μU of SCDase in 20 μl of 25 mM phosphate buffer, pH 7.0, containing 0.1% Triton X-100. When eicosapentaenoic acid (EPA) and docosahexaenoic acid (DHA) were used as a substrate, 120 μU of SCDase was used for the reaction. After incubation, reaction efficiencies were determined as described previously (23). Values are means for duplicate determinations. B: Electrospray ionization-liquid chromatography-mass spectrometry analyses were conducted with an API 365 mass spectrometer using the positive-ion mode. C: Fatty acid methyl esters of reconstructed GM1a were analyzed by gas chromatography (GC-14A; Shimadzu Co., Kyoto, Japan) with a flame-ionization detector and a capillary column (HR-SS-10, 0.25 mm × 30 m; Shinwa Chemical Industries, Kyoto, Japan). C18:0-GM1a, GM1a with stearic acid; C18:1-GM1a, GM1a with oleic acid; C18:2-GM1a, GM1a with linoleic acid; C18:3-GM1a, GM1a with α-linolenic acid; C20:5-GM1a, GM1a with eicosapentaenoic acid; C22:6-GM1a, GM1a with docosahexaenoic acid.

## RESULTS

### Condensation of various fatty acids to lyso-GM1a by SCDase and identification of the reconstructed GM1a

The extent of GM1a synthesis with unsaturated fatty acid was examined using the condensation reaction of SCDase. The efficiencies of all reactions reached ~80% when stearic acid (C18:0), oleic acid (C18:1), linoleic acid (C18:2), or α-linolenic acid (C18:3) was used as a substrate, whereas the value was 20–30% when eicosapentaenoic acid (C20:5) or docosahexaenoic acid (C22:6) was used (**Fig. 1A**). The saturated fatty acyl chains of C12-C18 were well condensed, but those of C2-C6 and C22-C26 were less condensed to lyso-GM1a by SCDase (23). These results suggest that the length of fatty acyl chains is more important in determining the efficiency of the condensation reaction by the SCDase than is the degree of unsaturation of the fatty acid, if the reaction period is long enough with an excess amount of enzyme. After the purification of the reconstructed GM1a, as described in Materials and Methods, the structure of GM1a was determined by ESI-LC-MS using the positive-ion mode. As shown in Fig. 1B, the characteristic pseudomolecular ions $(M+H)^+$ and $(M+Na)^+$ were found at values of the expected molecular masses corresponding to the reconstructed GM1a with a different fatty acid. Furthermore, the fatty acid molecule of each reconstructed GM1a was determined by gas chromatography after methanolysis of the sample. It was confirmed that each reconstructed GM1a contains the expected single fatty acid (Fig. 1C). These results clearly indicated that unsaturated fatty acids were successfully condensed by the SCDase to lyso-GM1a to generate a GM1a having each unsaturated fatty acid.

### Growth inhibition of Neuro2a cells by the GM1a reconstructed with unsaturated fatty acids

The addition of GM1a composed of d18:1 sphingosine and a stearic acid (C18:0-GM1a) or an oleic acid (C18:1-GM1a), both of which are naturally occurring gangliosides, did not affect the incorporation of [$^3$H]thymidine by Neuro2a cells (**Fig. 2A**). On the other hand, this index

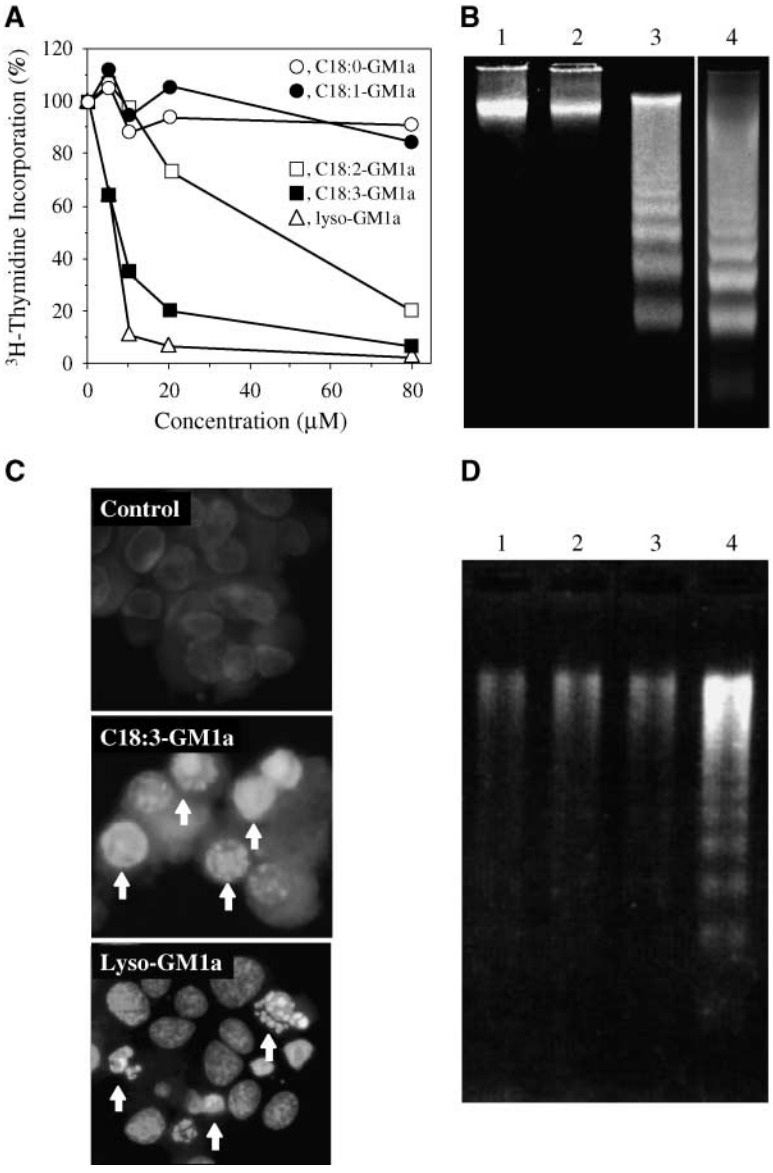


**Fig. 2.** Apoptosis of Neuro2a cells induced by C18:3-GM1a and lyso-GM1a. A: Growth inhibition of Neuro2a cells induced by GM1a reconstructed with unsaturated fatty acids or lyso-GM1a. Cells were treated with each GM1a at the concentrations indicated, and [$^3$H]thymidine incorporation was measured as described previously (28). B: DNA fragmentation of Neuro2a cells induced by C18:3-GM1a or lyso-GM1a. Neuro2a cells were incubated at 37°C for 24 h with 40 μM C18:0-GM1a, C18:3-GM1a, and lyso-GM1a. Fragmented DNA was then extracted and analyzed by 2% agarose gel electrophoresis. Lane 1, without GM1a; lane 2, C18:0-GM1a; lane 3, C18:3-GM1a; lane 4, lyso-GM1a. C: Chromatin condensation and nuclear fragmentation of Neuro2a cells induced by C18:3-GM1a and lyso-GM1a. An aliquot of Neuro2a cells after treatment with 40 μM gangliosides for 24 h was subjected to Hoechst 33258 staining. Arrows indicate the cells with condensed chromatin. D: DNA fragmentation of HL60 cells induced by C18:3-GM1a. HL60 cells were incubated at 37°C for 24 h with 10–20 μM C18:0-GM1a, and C18:3-GM1a. Fragmented DNA was then extracted and analyzed by 2% agarose gel electrophoresis. Lane 1, 10 μM C18:0-GM1a; lane 2, 20 μM C18:0-GM1a; lane 3, 10 μM C18:3-GM1a; lane 4, 20 μM C18:3-GM1a.

was markedly decreased in a dose-dependent manner by the addition of C18:2- and C18:3-GM1a, the Cer of which is composed of a d18:1 sphingosine and a linoleic acid (C18:2) and α-linolenic acid (C18:3), respectively. As shown previously (28), lyso-GM1a, which lacks the fatty acyl chain of GM1a, was very toxic to the cells (Fig. 2A).

### Features of apoptosis induced by C18:3-GM1a

Sueyoshi, Maehara, and Ito (28) demonstrated that lyso-GM1a induced apoptosis in Neuro2a cells. Thus, the possibility that the suppression of DNA synthesis by C18:3-GM1a is derived from apoptosis was examined. After treatment of cells with C18:3-GM1a, the genomic DNA showed a ladder fragmentation pattern on agarose gel electrophoresis, which is one of the features typical of apoptosis (Fig. 2B). In addition, C18:3-GM1a-treated cells showed chromatin condensation and nuclear fragmentation after staining with Hoechst 33258 (Fig. 2C). These results indicated that not only lyso-GM1a but also C18:3-GM1a induced the apoptosis of Neuro2a cells. Because DNA fragmentation was observed not only in Neuro2a cells but also in human leukemia cell line HL60 cells (Fig. 2D), the C18:3-GM1a-induced apoptosis is not specific for neuronal cells. Apoptotic cells were also quantified with a flow cytometer. The ratio of apoptotic cells reached 30% of total cells after treatment with C18:3-GM1a for 24 h (**Fig. 3E**), whereas it was less than 10% with C18:0-GM1a (Fig. 3C). Interestingly, after the removal of loosely bound GM1a by BSA treatment, apoptosis was still observed at almost the same rate (Fig. 3D). These results indicated that treatment with C18:3-GM1a, but not C18:0-GM1a, significantly induced apoptosis in Neuro2a cells.

Next, caspase activity was measured using the fluorescence substrate Ac-DEVD-MCA, which is specifically hydrolyzed by caspase-3. In Neuro2a cells, an increase of caspase-3-like activity was observed after the addition of C18:3-GM1a followed by incubation at 37°C for 18–24 h (**Fig. 4A**). Simultaneously, a DNA ladder was detected by agarose gel electrophoresis (Fig. 4B). The addition of an inhibitor for caspases, zVAD-fmk, to the Neuro2a cell culture inhibited the increase in protease activity (Fig. 4A) but not the DNA fragmentation (Fig. 4B). This result suggested that a caspase-3-independent signaling pathway is involved in the C18:3-GM1a-induced apoptosis.

### Incorporation and distribution of exogenously added gangliosides in Neuro2a cells

To quantify the amount of gangliosides that enter the Neuro2a cells, cell-bound gangliosides were determined after removing the loosely bound gangliosides by treatment of the cells with fatty acid-free BSA. The amounts of C18:0-GM1a, C18:3-GM1a, and lyso-GM1a bound to cells decreased to half after BSA treatment, suggesting that half of the gangliosides/lysogangliosides were attached loosely to cells (**Fig. 5A**). The amount of C18:3-GM1a incorporated in the cells was almost the same as that of C18:0-GM1a and was approximately twice that of lyso-GM1a after BSA treatment. It is noted that the incorporation of gangliosides increased slowly during the course of incubation

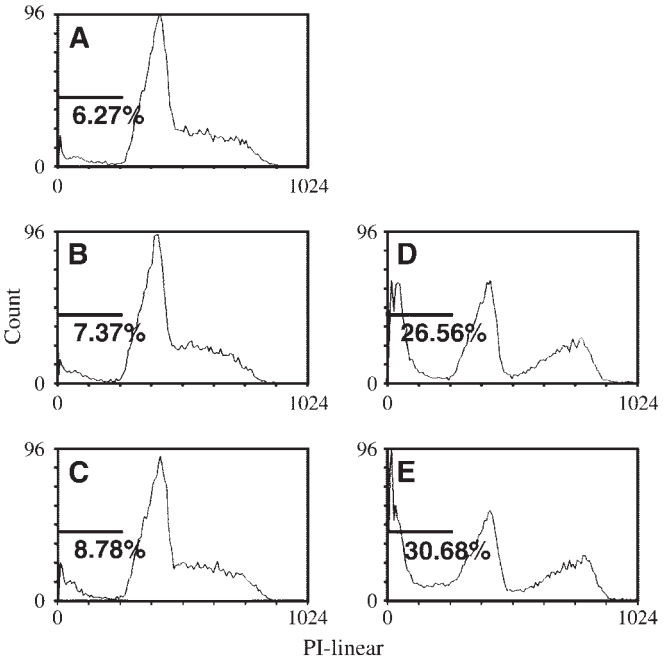


**Fig. 3.** Quantification of apoptosis in Neuro2a cells with a flow cytometer. In C and E, cells were treated with 40 μM C18:0-GM1a and C18:3-GM1a, respectively, for 24 h in serum-free DMEM containing 20 μg/ml BSA and the N-2 supplement. In B and D, cells were treated with 40 μM C18:0-GM1a and C18:3-GM1a, respectively, and washed with DMEM containing 0.2% fatty acid-free BSA to remove loosely bound GM1a at 6 h and then recultured in serum-free DMEM containing 20 μg/ml BSA and the N-2 supplement for 18 h. The DNA fragmentations were quantified using a flow cytometer. Numbers represent the percentages of apoptotic cells. Control (A) represents the percentage of apoptotic cells without treatment with gangliosides after 24 h. PI, propridium iodide.

regardless of the difference in the fatty acyl chain (Fig. 5A). The distribution of exogenously added gangliosides in cells was compared with and without treatment with BSA by confocal laser-scanning microscopy after staining with biotin-labeled CTB (Fig. 5B). It is noteworthy that both C18:0- and C18:3-GM1a were detected mainly on the cell surface (arrows) and partly in intracellular compartments (arrowheads) during incubation, regardless of the treatment of cells with BSA. At the cell surface but not at the intracellular compartment, gangliosides were found to decrease in quantity on treatment of the cells with BSA, consistent with the result shown in Fig. 5A. This result confirmed that loosely bound, but not incorporated, gangliosides were removed by BSA treatment. Apoptosis could be caused by the C18:3-GM1a incorporated into plasma membranes, because apoptosis was induced after treatment of the cells with BSA (Fig. 3), although the possibility that C18:3-GM1a incorporated into intracellular compartments could cause the apoptosis cannot be ruled out at present.

### Metabolism of exogenously added C18:0-GM1a and C18:3-GM1a in Neuro2a cells

To investigate how GM1a is metabolized in Neuro2a cells after its incorporation, $^{14}$C-labeled C18:0- and C18:3-

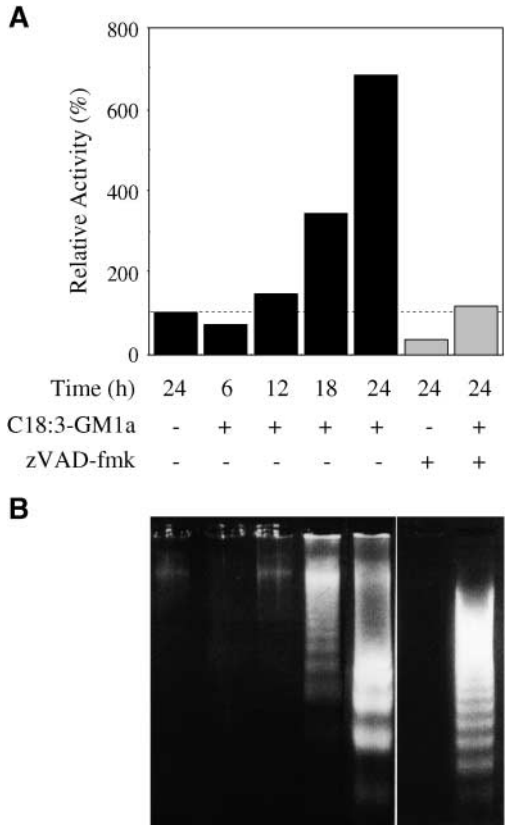


**Fig. 4.** Activation of caspase-3-like enzymes by C18:3-GM1a. A: Time course of caspase-3-like activity. Neuro2a cells were incubated in DMEM containing the N-2 supplement and 20 μg/ml BSA at 37°C with 40 μM C18:3-GM1a in the presence or absence of zVAD-fmk, a specific inhibitor of caspases, for the times indicated. Cytosolic extracts were prepared from cells, and the caspase-3-like activity in the lysates was measured using the fluorescent substrate Ac-DEVD-MCA. The fluorescence of the cleaved substrates was determined using a microplate reader (CS-9300PC; Shimadzu Co., Kyoto, Japan) set at an excitation wavelength of 360 nm and an emission wavelength of 460 nm. B: Time course for genomic DNA fragmentation. Genomic DNA was extracted from the cells and then analyzed by electrophoresis. Details are described in Materials and Methods.

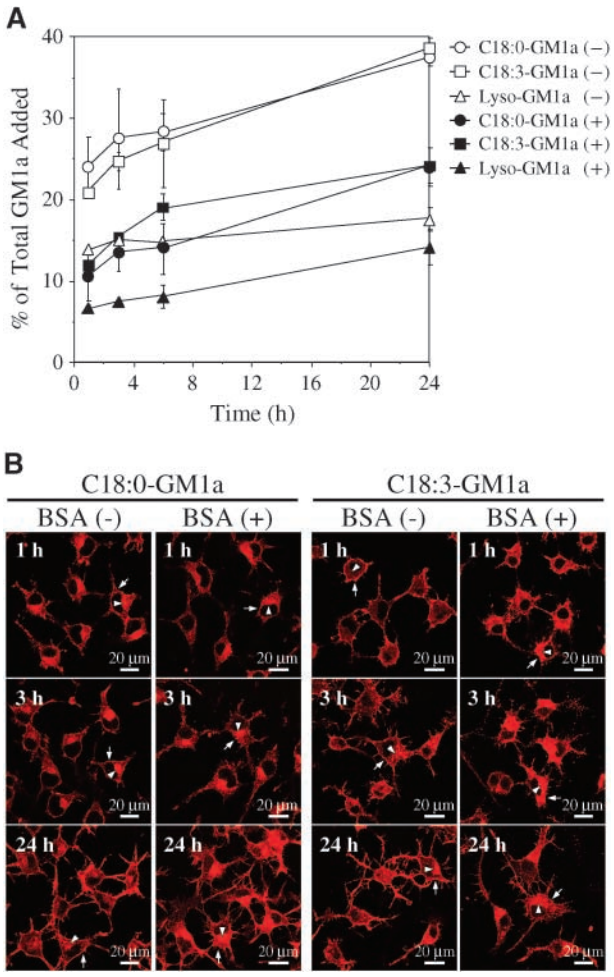


**Fig. 5.** Incorporation of GM1a in Neuro2a cells. A: Cells ($1 \times 10^5$) were incubated with 40 μM C18:0-GM1a, C18:3-GM1a, and lyso-GM1a at 37°C for the times indicated. After treatment of the cells with 0.2% fatty acid-free BSA solution, lipids were extracted from cells and then analyzed by TLC using chloroform/methanol/0.02% $CaCl_2$ (5:4:1, v/v). For the control experiment, the BSA treatment was omitted. B: Cells were treated with 40 μM C18:0-GM1a and C18:3-GM1a for the indicated times. After incubation with gangliosides, cells were treated with (BSA+) or without (BSA−) 0.2% fatty acid-free BSA solution and then stained with biotin-labeled cholera toxin B-subunit (CTB). Signals were observed by confocal laser-scanning microscopy as described in Materials and Methods. Values are expressed as the mean with SD (n = 3).

GM1a (labeled at fatty acyl chains) were added to the cell cultures. Both $^{14}$C-labeled GM1a forms were incorporated into Neuro2a cells and partially metabolized to GM2, GM3, and more complex gangliosides, mainly GD1a (**Fig. 6**). The metabolic patterns of the two $^{14}$C-labeled GM1a forms were almost the same, although the metabolic rate of C18:3-GM1a was slower than that of C18:0-GM1a. It is noted that neither GM1a was metabolized to Cer under the conditions used, which are known to induce apoptosis, indicating that apoptosis was not induced by Cer generated from the metabolism of C18:3-GM1a.

### Different effects of C18:3-GM1a and lyso-GM1a on erythrocytes and MAPKs

The apparent features of the apoptosis induced by C18:3-GM1a seem to be almost the same as, if not identical to, those caused by lyso-GM1a (28). Therefore, it was investigated whether or not the mechanisms underlying the apoptosis induced by C18:3-GM1a and lyso-GM1a are the same. As shown in **Fig. 7A**, lyso-GM1a caused the hemolysis of sheep erythrocytes in a dose-dependent manner, whereas C18:0-GM1a and C18:3-GM1a did not. This result may indicate that the lyso-GM1a-induced apoptosis of Neuro2a cells is caused by a nonspecific detergent-like effect, perhaps by physical damage to the plasma membranes, and is different from the apoptosis induced by C18:3-GM1a.

Neuritogenesis of Neuro2a cells was induced by adding gangliosides in which the activation of MAPK was observed (41). Considering this report, the involvement of MAPK activation in C18:3-GM1a-induced apoptosis was examined. The treatment of Neuro2a cells with lyso-GM1a decreased the phosphorylation level of ERK1/2 and simultaneously increased that of SAPK/JNK (Fig. 7B). On the

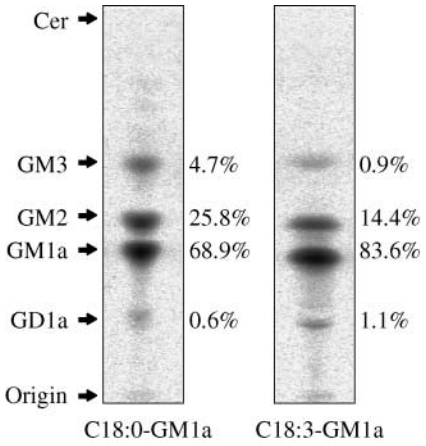


**Fig. 6.** Intracellular metabolism of C18:0-GM1a and C18:3-GM1a in Neuro2a cells. Cells ($1 \times 10^6$) were incubated in DMEM containing the N-2 supplement and 20 μg/ml BSA at 37°C for 24 h with $^{14}$C-labeled C18:0-GM1a or C18:3-GM1a (2.2 μCi, 40 μM). After the incubation, total lipids were extracted, separated by TLC using chloroform/methanol/0.02% $CaCl_2$ (5:4:1, v/v), and then analyzed using an imaging analyzer (BAS1500; Fuji Film, Tokyo, Japan). Cer, ceramide.

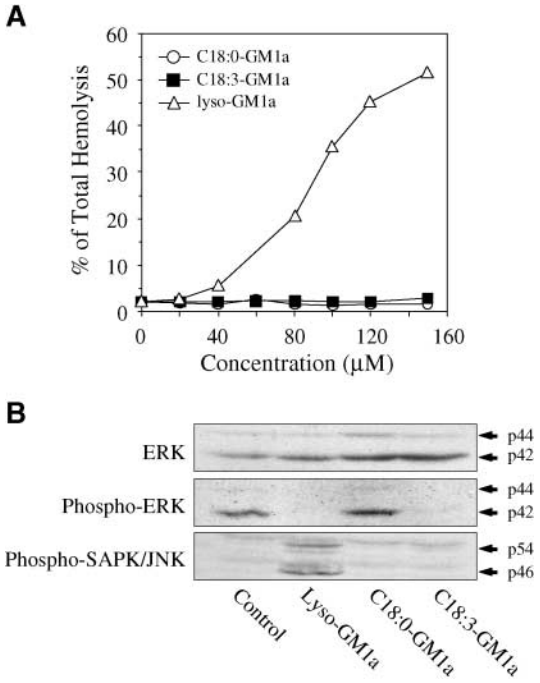


**Fig. 7.** Differential effects of C18:3-GM1a and lyso-GM1a in sheep erythrocytes and mitogen-activated protein kinases (MAPKs). A: Intact sheep erythrocytes were incubated in phosphate-buffered saline, pH 7.4, with the indicated concentrations of C18:0-GM1a, C18:3-GM1a, and lyso-GM1a for 30 min at 37°C. The reaction mixtures were centrifuged, and the supernatants were measured spectrophotometrically for hemoglobin at 540 nm using a microplate photometer. Total hemolysis was performed with 0.5% Triton X-100. B: Neuro2a cells ($1 \times 10^6$) were incubated in DMEM containing the N-2 supplement and 20 μg/ml BSA at 37°C for 1 h with 40 μM GM1a, and then cytosolic extracts were prepared from the cells. The phosphorylation of MAPK was detected by Western blotting using specific polyclonal antibodies. Details are given in Materials and Methods. ERK, extracellular signal-regulated kinase; SAPK/JNK, stress-activated protein kinase/c-Jun N-terminal kinase.

other hand, C18:3-GM1a did not affect the phosphorylation of SAPK/JNK, although it decreased that of ERK1/2 similar to lyso-GM1a (Fig. 7B). C18:0-GM1a did not cause any change in the activity of MAPKs under the conditions used. Another MAPK, p38 MAPK, was not affected by the addition of either C18:3-GM1a or lyso-GM1a (data not shown).

### Distribution of exogenously added gangliosides in lipid microdomains

In the sucrose density gradient analysis, endogenous GSLs, including GM2 and GM1a, were concentrated mainly in DIM fractions (**Fig. 8A**, fractions 2–4). The exogenously added C18:0-GM1a and C18:3-GM1a were detected mainly in bulk membrane-lipid fractions (Fig. 8B, fractions 6–8) and partly in DIM fractions (Fig. 8B, fractions 2–4) without treatment of the cells with BSA. However, after the removal of loosely bound GM1a by BSA, half of the GM1a was detected in DIM fractions, indicating that the incorporated GM1a, but not loosely bound GM1a, was concentrated in lipid microdomains similar to endogenous GM1a (Fig. 8C, fractions 2–4). Interestingly, the behavior of C18:3-GM1a in the sucrose density gradient was almost the same of that of C18:0-GM1a but completely different from that of lyso-GM1a, which was not detected in DIM fractions and was distributed only in bulk membrane-lipid fractions (Fig. 8A, fractions 6–8). In summary, C18:3-GM1a was incorporated and distributed in cell membranes possibly in the same manner as C18:0-GM1a and concentrated in DIM fractions after its incorporation, similar to endogenous GSLs, whereas lyso-GM1a was detected solely in bulk membrane lipid fractions.

### Effects of C18:3-GM1a and lyso-GM1a on lipid microdomains

NCAM-120, a member of the immunoglobulin superfamily that is expected to be localized to lipid microdomains of neuronal cells (42), was analyzed by Western blotting using a specific monoclonal antibody after the treatment of cells with gangliosides. It was found that NCAM-120 was completely excluded from DIM fractions of lyso-GM1a-treated cells but was included in the fractions of C18:3-GM1a-treated cells when DIM was prepared by the sucrose density gradient method using Triton X-100 (**Fig. 9A**). However, when the membrane was fractionated using an OptiPrep density gradient without detergents, NCAM-120 disappeared from the low-density fractions and could only be detected in high-density fractions in both lyso-GM1a- and C18:3-GM1a-treated cells (Fig. 9B). C18:0-GM1a did not affect the distribution of NCAM-120 in sucrose or OptiPrep density gradients. These results suggested that the addition of lyso-GM1a to the Neuro2a culture almost completely disrupts the structure of the lipid microdomains (DIM fractions), whereas C18:3-GM1a does not disrupt but somehow affects the structure, judging from the behavior of a lipid microdomain-associated protein, NCAM-120, in sucrose and OptiPrep density gradients. In contrast to these aberrant gangliosides, naturally occurring C18:0-GM1a has no apparent effect on the structure of

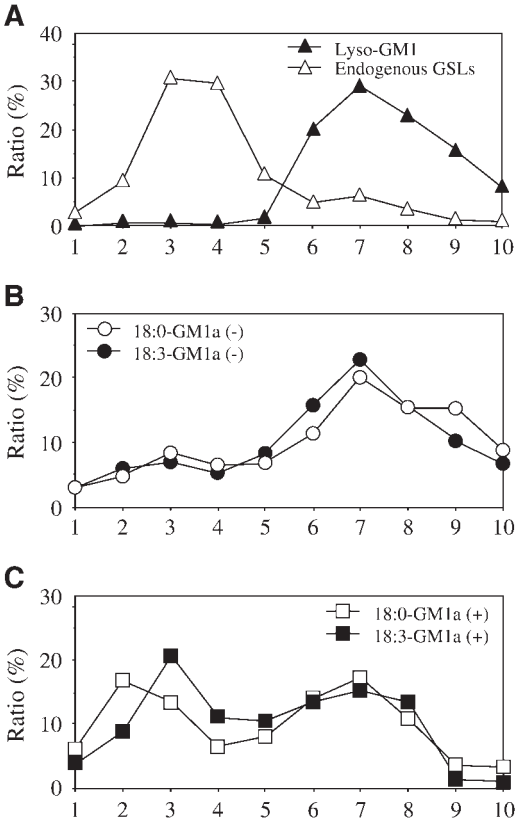


**Fig. 8.** Effects on the distribution of GM1a in density gradient centrifugation. Cells ($1 \times 10^6$) were incubated in DMEM containing the N-2 supplement and 20 μg/ml BSA at 37°C for 1 h with 40 μM GM1a. After the GM1a treatment, cells were washed with DMEM containing 0.2% fatty acid-free BSA (C) or not washed (A, B), homogenized in 1% Triton X-100-containing lysis buffer, and subjected to sucrose density gradient centrifugation. The centrifuged samples were divided into 10 fractions that were subjected to TLC. GM1a/lyso-GM1a and endogenous glycosphingolipids (GSLs) were detected by TLC blotting using biotin-labeled CTB and orcinol-$H_2SO_4$, respectively, as described in Materials and Methods. Values represent percentages of GSLs in each fraction.

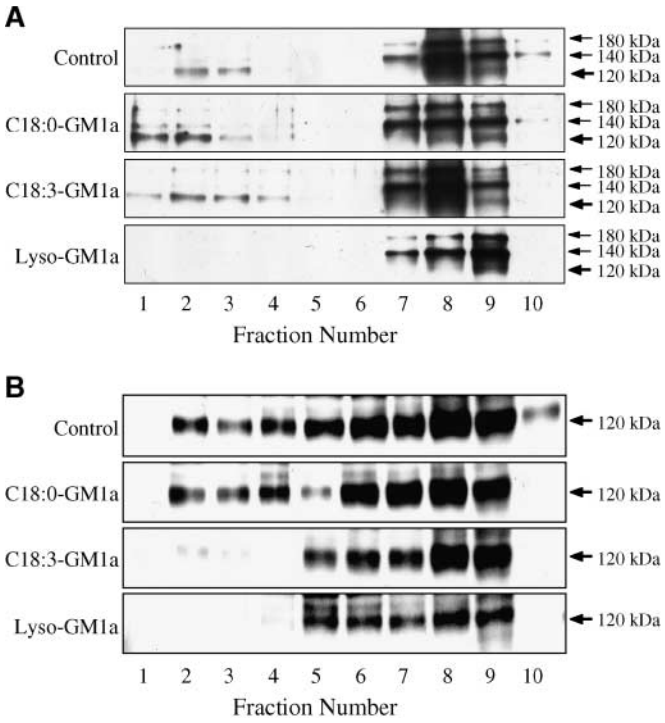


**Fig. 9.** Effects on the distribution of glycosylphosphatidylinositol-anchored proteins in density gradient centrifugation. Cells ($1 \times 10^6$) were incubated in DMEM containing the N-2 supplement and 20 μg/ml BSA at 37°C for 1 h with 40 μM of each GM1a, and then the membrane was fractionated by two different density gradient centrifugations. A: Sucrose density gradient. After the GM1a treatment, cells were homogenized in 1% Triton X-100-containing lysis buffer and subjected to sucrose density gradient centrifugation. B: OptiPrep density gradient. After the GM1a treatment, cells were homogenized in detergent-free lysis buffer and subjected to OptiPrep density gradient centrifugation. After the centrifugation, samples were divided into 10 fractions that were subjected to SDS-PAGE, and neural cell adhesion molecule (NCAM) was detected by Western blotting. The 120 kDa isoform of NCAM is a glycosylphosphatidylinositol-anchored protein. Details are given in Materials and Methods.

lipid microdomains when added to the cell culture at a concentration of 40 μM (Fig. 9A, B).

## DISCUSSION

It is generally accepted that gangliosides contain saturated fatty acids but not PUFAs in the Cer moiety. Unexpectedly, we found in the literature that PUFAs are widely distributed in the gangliosides as a minor constituent [e.g., mouse fibroblast l cells contain 1.3% and 7.2% of PUFAs in the fatty acid portion of monosialoganglioside and disialoganglioside, respectively (32); bovine serum contains 1.7% and 1.1% of C18:3 fatty acids in monosialoganglioside and disialoganglioside, respectively (32); human milk contains 0.39% and 0.17% of α-linolenic acid in GM3 and GD3, respectively (33); and GD3 of bovine kidney contains ~2% of C18:3 fatty acid (31)]. Nevertheless, little attention has been paid to the physiological significance of PUFA-containing gangliosides. We found that C18:3-GM1a at relatively high concentration (<40 μM) induced apoptosis in Neuro2a cells, whereas at lower concentration (5 μM) it induced neurite formation of PC12 cells in the absence of nerve growth factor (data not shown). Considering these results and the ubiquitous distribution of PUFA-containing gangliosides, the physiological and pharmacological functions of PUFA-containing gangliosides should be further clarified not only in vitro but also in vivo. In this context, a series of reports demonstrating that remodeling of the fatty acyl chain of GM1a enhanced the neuroprotective effects is particularly interesting (43, 44).

In the apoptosis induced by C18:3-GM1a, a caspase-3-independent signaling pathway could be involved, because the addition of an inhibitor for caspases, zVZD-fmk, to the Neuro2a cell culture inhibited the increase in the protease activity but not the DNA fragmentation. A pathway that is not inhibited by zVAD-fmk has also been observed in lyso-GM1a-induced apoptosis in Neuro2a cells (28) and

adenovirus death factor-induced apoptosis (45). Recently, it was reported that endonuclease G released from mitochondria was involved in caspase-independent DNA degradation in the apoptosis of mouse embryonic fibroblasts, which lack the caspase-activated DNase (46). Thus, it is likely that endonuclease G-like enzymes along with caspase-like enzymes are involved in the C18:3-GM1a- and lyso-GM1a-induced DNA fragmentation in Neuro2a cells. It should be noted that zVAD-fmk does not affect the activity of endonuclease G.

The activation of the SAPK/JNK cascade seems to be essential for apoptosis induced by stress, including ionizing radiation and chemotherapeutic drugs (47, 48). On the other hand, the activation of ERK promotes cell proliferation. The balance of the activation between the SAPK/JNK and ERK pathways is thought to determine the fate of cells (i.e., death or survival) (49, 50). In this context, it is interesting that the inhibition of ERK (inhibition of the ERK pathway) was caused by both C18:3-GM1a and lyso-GM1a, whereas the activation of SAPK/JNK was attributable only to lyso-GM1a. SAPK seems to be activated through the nonspecific stress applied to the plasma membranes by lyso-GM1a but not C18:3-GM1a, although the mechanism underlying the apoptosis induced by both aberrant gangliosides remains to be clarified.

Recently, GSLs were found to be enriched with cholesterol to form lipid microdomains on plasma membranes (12). It is believed that the difference in the hydrophobic region of glycerophospholipids and sphingolipids (i.e., the former contains mainly unsaturated fatty acids and the latter mainly saturated fatty acids) causes the phase separation to form lipid microdomains (21, 51). C18:3-GM1a, which contains polyunsaturated fatty acid, was expected to be excluded from lipid microdomains. Unexpectedly, however, C18:3-GM1a was found in DIM fractions at almost the same level as C18:0-GM1a. This result can be explained by either the "hydrogen bonding network hypothesis," in which sphingolipids are considered to bind each other with hydrogen bonds between hydroxy and amido groups, or the "polar head group interaction hypothesis," in which GSLs are considered to aggregate via lateral carbohydrate-carbohydrate interactions (52). It is noteworthy that lyso-GM1a was not detected in DIM fractions, possibly because the lipid destroyed the structure of lipid microdomains.

To address the significance of the fatty acid moiety of GSLs, a specific and convenient method is still required to reconstruct GSLs with unsaturated fatty acids. Until now, the only choice was a chemical procedure (53) that could generate by-products and is time-consuming. SCDase, an enzyme capable of hydrolyzing the *N*-acyl linkage between fatty acid and Cer in various GSLs and sphingomyelin (22), was found to catalyze the reverse reaction, in which a fatty acid is condensed to a lyso-GSL to yield a GSL (23). Cloning of SCDase from *Shewanella alga* G8 revealed that the reversible reactions were catalyzed by a single protein (54). SCDase is a superior reagent for remodeling GSLs with not only saturated fatty acids (37, 55, 56) but also unsaturated fatty acids (this study). Thus, the method using SCDase to remodel fatty acyl chains in gangliosides will facilitate further development in GSL research.

The authors thank H. Izu (Takara Bio Co. Ltd.) for ESI-LC-MS analysis. This work was supported by a Grant-in-Aid for Scientific Research on Priority Areas (12140204) and Basic Research B (15380073) from the Ministry of Education, Culture, Sports, Science, and Technology of Japan.

## REFERENCES

1. Tsuji, S., M. Arita, and Y. Nagai. 1983. GQ1b, a bioactive ganglioside that exhibits novel nerve growth factor (NGF)-like activities in the two neuroblastoma cell lines. *J. Biochem. (Tokyo)*. **94:** 303–306.
2. Bremer, E. G., J. Schlessinger, and S. Hakomori. 1986. Ganglioside-mediated modulation of cell growth. Specific effects of GM3 on tyrosine phosphorylation of the epidermal growth factor receptor. *J. Biol. Chem.* **261:** 2434–2440.
3. Nojiri, H., F. Takaku, Y. Terui, Y. Miura, and M. Saito. 1986. Ganglioside GM3: an acidic membrane component that increases during macrophage-like cell differentiation can induce monocytic differentiation of human myeloid and monocytoid leukemic cell lines HL-60 and U937. *Proc. Natl. Acad. Sci. USA*. **83:** 782–786.
4. Mutoh, T., A. Tokuda, T. Miyadai, M. Hamaguchi, and N. Fujiki. 1995. Ganglioside GM1 binds to the Trk protein and regulates receptor function. *Proc. Natl. Acad. Sci. USA*. **92:** 5087–5091.
5. Wu, G., and R. W. Ledeen. 1991. Stimulation of neurite outgrowth in neuroblastoma cells by neuraminidase: putative role of GM1 ganglioside in differentiation. *J. Neurochem.* **56:** 95–104.
6. Hakomori, S., and Y. Igarashi. 1993. Gangliosides and glycosphingolipids as modulators of cell growth, adhesion, and transmembrane signaling. *Adv. Lipid Res.* **25:** 147–162.
7. Karlsson, K. A. 1989. Animal glycosphingolipids as membrane attachment sites for bacteria. *Annu. Rev. Biochem.* **58:** 309–350.
8. Hakomori, S., and Y. Igarashi. 1995. Functional role of glycosphingolipids in cell recognition and signaling. *J. Biochem. (Tokyo)*. **118:** 1091–1103.
9. Hakomori, S., K. Handa, K. Iwabuchi, S. Yamamura, and A. Prinetti. 1998. New insights in glycosphingolipid function: "glycosignaling domain," a cell surface assembly of glycosphingolipids with signal transducer molecules, involved in cell adhesion coupled with signaling. *Glycobiology.* **8:** xi–xix.
10. Okada, Y., G. Mugnai, E. G. Bremer, and S. Hakomori. 1984. Glycosphingolipids in detergent-insoluble substrate attachment matrix (DISAM) prepared from substrate attachment material (SAM). Their possible role in regulating cell adhesion. *Exp. Cell Res.* **155:** 448–456.
11. Iwabuchi, K., S. Yamamura, A. Prinetti, K. Handa, and S. Hakomori. 1981. GM3-enriched microdomain involved in cell adhesion and signal transduction through carbohydrate-carbohydrate interaction in mouse melanoma B16 cells. *J. Biol. Chem.* **273:** 9130–9138.
12. Simons, K., and E. Ikonen. 1997. Functional rafts in cell membranes. *Nature.* **387:** 569–572.
13. Brown, D. A., and J. K. Rose. 1992. Sorting of GPI-anchored proteins to glycolipid-enriched membrane subdomains during transport to the apical cell surface. *Cell.* **68:** 533–544.
14. Brown, D. A., and E. London. 2000. Structure and function of sphingolipid- and cholesterol-rich membrane rafts. *J. Biol. Chem.* **275:** 17221–17224.
15. Bieberich, E., S. MacKinnon, J. Silva, and R. K. Yu. 2001. Regulation of apoptosis during neuronal differentiation by ceramide and b-series complex gangliosides. *J. Biol. Chem.* **276:** 44396–44404.
16. Svennerholm, L. 1994. Gangliosides—a new therapeutic agent against stroke and Alzheimer's disease. *Life Sci.* **55:** 2125–2134.
17. Schneider, J. S., D. P. Roeltgen, D. S. Rothblat, J. Chapas-Crilly, L. Seraydarian, and J. Rao. 1995. GM1 ganglioside treatment of Parkinson's disease: an open pilot study of safety and efficacy. *Neurology.* **45:** 1149–1154.
18. Geisler, F. H., D. C. Dorsey, and W. P. N. Coleman. 1991. Recovery of motor function after spinal-cord injury—a randomized, placebo-controlled trial with GM-1 ganglioside. *N. Engl. J. Med.* **324:** 1829–1838.

19. Avrova, N. F., and S. A. Zabelinskii. 1971. Fatty acids and long chain bases of vertebrate brain gangliosides. *J. Neurochem.* **18:** 675–681.
20. Bittman, R., C. R. Kasireddy, P. Mattjus, and J. P. Slotte. 1994. Interaction of cholesterol with sphingomyelin in monolayers and vesicles. *Biochemistry.* **33:** 11776–11781.
21. Smaby, J. M., M. Momsenk, V. S. Kulkarni, and R. E. Brown. 1996. Cholesterol-induced interfacial area condensations of galactosylceramides and sphingomyelins with identical acyl chains. *Biochemistry.* **35:** 5696–5704.
22. Ito, M., T. Kurita, and K. Kita. 1995. A novel enzyme that cleaves the *N*-acyl linkage of ceramides in various glycosphingolipids as well as sphingomyelin to produce their lyso forms. *J. Biol. Chem.* **270:** 24370–24374.
23. Kita, K., T. Kurita, and M. Ito. 2001. Characterization of the reversible nature of the reaction catalyzed by sphingolipid ceramide *N*-deacylase. A novel form of reverse hydrolysis reaction. *Eur. J. Biochem.* **268:** 592–602.
24. Miyatake, T., and K. Suzuki. 1972. Globoid cell leukodystrophy: additional deficiency of psychosine galactosidase. *Biochem. Biophys. Res. Commun.* **48:** 539–543.
25. Svennerholm, L., M. T. Vanier, and J. E. Mansson. 1980. Krabbe disease: a galactosylsphingosine (psychosine) lipidosis. *J. Lipid Res.* **21:** 53–64.
26. Igisu, H., and K. Suzuki. 1984. Progressive accumulation of toxic metabolite in a genetic leukodystrophy. *Science.* **224:** 753–755.
27. Toda, K., T. Kobayashi, I. Goto, T. Kurokawa, and K. Ogomori. 1989. Accumulation of lysosulfatide (sulfogalactosylsphingosine) in tissues of a boy with metachromatic leukodystrophy. *Biochem. Biophys. Res. Commun.* **159:** 605–611.
28. Sueyoshi, N., T. Maehara, and M. Ito. 2001. Apoptosis of Neuro2a cells induced by lysosphingolipids with naturally occurring stereochemical configurations. *J. Lipid Res.* **42:** 1197–1202.
29. Hannun, Y. A., and R. M. Bell. 1987. Lysosphingolipids inhibit protein kinase C: implications for the sphingolipidoses. *Science.* **235:** 670–674.
30. Kanazawa, T., S. Nakamura, M. Momoi, T. Yamaji, H. Takematsu, H. Yano, H. Sabe, A. Yamamoto, T. Kawasaki, and Y. Kozutsumi. 2000. Inhibition of cytokinesis by a lipid metabolite, psychosine. *J. Cell Biol.* **149:** 943–950.
31. Puro, K., and A. Keranen. 1969. Fatty acids and sphingosines of bovine-kidney gangliosides. *Biochim. Biophys. Acta.* **187:** 393–400.
32. Weinstein, D. B., J. B. Marsh, M. C. Glick, and L. Warren. 1970. Membranes of animal cells. VI. The glycolipids of the L cell and its surface membrane. *J. Biol. Chem.* **245:** 3928–3937.
33. Bode, L., C. Beermann, M. Mank, G. Kohn, and G. Boehm. 2004. Human and bovine milk gangliosides differ in their fatty acid composition. *J. Nutr.* **134:** 3016–3020.
34. Fukano, Y., and M. Ito. 1997. Preparation of GM1 ganglioside with sialidase-producing marine bacteria as a microbial biocatalyst. *Appl. Environ. Microbiol.* **63:** 1861–1865.
35. Ito, M., K. Kita, T. Kurita, N. Sueyoshi, and H. Izu. 2000. Enzymatic *N*-deacylation of sphingolipids. *Methods Enzymol.* **311:** 297–303.
36. Kurita, T., H. Izu, M. Sano, M. Ito, and I. Kato. 2000. Enhancement of hydrolytic activity of sphingolipid ceramide *N*-deacylase in the aqueous-organic biphasic system. *J. Lipid Res.* **41:** 846–851.
37. Mitsutake, S., K. Kita, T. Nakagawa, and M. Ito. 1998. Enzymatic synthesis of $^{14}$C-glycosphingolipids by reverse hydrolysis reaction of sphingolipid ceramide *N*-deacylase: detection of endoglycoceramidase activity in a seaflower. *J. Biochem. (Tokyo).* **123:** 859–863.
38. Laemmli, U. K. 1970. Cleavage of structural proteins during the assembly of the head of bacteriophage T4. *Nature.* **227:** 680–685.
39. Rodgers, W., and J. K. Rose. 1996. Exclusion of CD45 inhibits activity of p56lck associated with glycolipid-enriched membrane domains. *J. Cell Biol.* **135:** 1515–1523.
40. Smart, E. J., Y. S. Ying, C. Mineo, and R. G. Anderson. 1995. A detergent-free method for purifying caveolae membrane from tissue culture cells. *Proc. Natl. Acad. Sci. USA.* **92:** 10104–10108.
41. Prinetti, A., K. Iwabuchi, and S. Hakomori. 1999. Glycosphingolipid-enriched signaling domain in mouse neuroblastoma Neuro2a cells. Mechanism of ganglioside-dependent neuritogenesis. *J. Biol. Chem.* **274:** 20916–20924.
42. Kramer, E. M., C. Klein, T. Koch, M. Boytinck, and J. Trotter. 1999. Compartmentation of Fyn kinase with glycosylphosphatidylinositol-anchored molecules in oligodendrocytes facilitates kinase activation during myelination. *J. Biol. Chem.* **274:** 29042–29049.
43. Manev, H., M. Favaron, S. Vicini, A. Guidotti, and E. Costa. 1990. Glutamate-induced neuronal death in primary cultures of cerebellar granule cells: protection by synthetic derivatives of endogenous sphingolipids. *J. Pharmacol. Exp. Ther.* **252:** 419–427.
44. Kharlamov, A., A. Guidotti, E. Costa, R. Hayes, and D. Armstrong. 1993. Semisynthetic sphingolipids prevent protein kinase C translocation and neuronal damage in the perifocal area following a photochemically induced thrombotic brain cortical lesion. *J. Neurosci.* **13:** 2483–2494.
45. Lavoie, J. N., M. Nguyen, R. C. Marcellus, P. E. Branton, and G. C. Shore. 1998. E4orf4, a novel adenovirus death factor that induces p53-independent apoptosis by a pathway that is not inhibited by zVAD-fmk. *J. Cell Biol.* **140:** 637–645.
46. Li, L. Y., X. Luo, and X. Wang. 2001. Endonuclease G is an apoptotic DNase when released from mitochondria. *Nature.* **412:** 95–99.
47. Verheij, M., R. Bose, X. H. Lin, B. Yao, W. D. Jarvis, S. Grant, M. J. Birrer, E. Szabo, L. I. Zon, J. M. Kyriakis, et al. 1996. Requirement for ceramide-initiated SAPK/JNK signalling in stress-induced apoptosis. *Nature.* **380:** 75–79.
48. Zanke, B. W., K. Boudreau, E. Rubie, E. Winnett, L. A. Tibbles, L. Zon, J. Kyriakis, F. F. Liu, and J. R. Woodgett. 1996. The stress-activated protein kinase pathway mediates cell death following injury induced by cis-platinum, UV irradiation or heat. *Curr. Biol.* **6:** 606–613.
49. Spiegel, S., O. Cuvillier, L. C. Edsall, T. Kohama, R. Menzeleev, Z. Olah, A. Olivera, G. Pirianov, D. M. Thomas, Z. Tu, et al. 1998. Sphingosine-1-phosphate in cell growth and cell death. *Ann. N. Y. Acad. Sci.* **845:** 11–18.
50. Jarvis, W. D., and S. Grant. 1998. The role of ceramide in the cellular response to cytotoxic agents. *Curr. Opin. Oncol.* **10:** 552–559.
51. Brown, D. A., and E. London. 1998. Functions of lipid rafts in biological membranes. *Annu. Rev. Cell Dev. Biol.* **14:** 111–136.
52. Masserini, M., and D. Ravasi. 2001. Role of sphingolipids in the biogenesis of membrane domains. *Biochim. Biophys. Acta.* **1532:** 149–161.
53. Kamio, K., S. Gasa, and A. Makita. 1992. Galactosylceramide containing omega-amino-fatty acids: preparation, characterization, and sulfotransferase acceptor. *J. Lipid Res.* **33:** 1227–1232.
54. Furusato, M., N. Sueyoshi, S. Mitsutake, K. Sakaguchi, K. Kita, N. Okino, S. Ichinose, A. Omori, and M. Ito. 2002. Molecular cloning and characterization of sphingolipid ceramide *N*-deacylase from a marine bacterium, *Shewanella alga* G8. *J. Biol. Chem.* **277:** 17300–17307.
55. Tani, M., K. Kita, H. Komori, T. Nakagawa, and M. Ito. 1998. Enzymatic synthesis of omega-amino-ceramide: preparation of a sensitive fluorescent substrate for ceramidase. *Anal. Biochem.* **263:** 183–188.
56. Nakagawa, T., M. Tani, K. Kita, and M. Ito. 1999. Preparation of fluorescence-labeled GM1 and sphingomyelin by the reverse hydrolysis reaction of sphingolipid ceramide *N*-deacylase as substrates for assay of sphingolipid-degrading enzymes and for detection of sphingolipid-binding proteins. *J. Biochem. (Tokyo).* **126:** 604–611.